THE JOURNAL OF PHYSICAL CHEMISTRY B
A JOURNAL OF THE AMERICAN CHEMICAL SOCIETY

pubs.acs.org/JPCB

Article

Porphyrin-Based Hybrid Nanohelices: Cooperative Effect between Molecular and Supramolecular Chirality on Amplified Optical Activity

Zakaria Anfar, Balamurugan Kuppan, Antoine Scalabre, Rahul Nag, Emilie Pouget, Sylvain Nlate, Gabriele Magna, Ilaria Di Filippo, Donato Monti, Mario L. Naitana, Manuela Stefanelli, Tatsiana Nikonovich, Victor Borovkov, Riina Aav, Roberto Paolesse, and Reiko Oda*

Cite This: *J. Phys. Chem. B* 2024, 128, 1550−1556

Read Online

ACCESS | Metrics & More | Article Recommendations | Supporting Information

ABSTRACT: The development of chiral receptors for discriminating the configuration of the analyte of interest is increasingly urgent in view of monitoring pollution in water and waste liquids. Here, we investigate an easy protocol to immobilize the desired non-water-soluble receptors inside a water-dispersible chiral nanoplatform made of silica. This approach induces chirality in the receptors and Here, we investigate an easy protocol to immobilize the desired non-water-soluble receptors inside a water-dispersible chiral nanoplatform made of silica. This approach induces chirality in the receptors and makes the dye@nanohelix system disperse in a suspension of water without aggregation. We noted strong induction and amplification of chiroptical activity in both achiral and chiral (proline-based or hemicucurbituril-based) porphyrin derivatives with and without zinc ions once confined and organized in nanometer silica helices. The results clearly demonstrated that the organization-induced chirality amplification of porphyrins dominates the molecular chirality, and the amplification is more efficient for more flexible porphyrins (especially free-base and achiral).

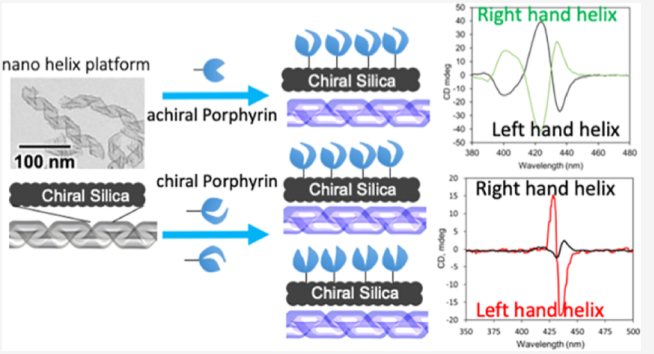

INTRODUCTION

The design and synthesis of chiral materials of diverse types[1] are continuously pursued for their use in various fields such as chiral induction, recognition, or amplification. Based on small chiral selectors of natural or synthetic origin, there has been important progress in recent years in the development of chiral inorganic materials,[2,3] which often display enhanced optical activities strictly related to their easily tunable morphology.[4] While still in its infancy, the line-up of different soft-templating assembly methods allowed for the preparation of materials with potential use in optoelectronic devices.[5] Other inorganic materials have also shown enantioselective recognition and sensing properties.[6,7] One of the hottest topics concerning the use of chiral recognition is undoubtedly found in the environment preservation and health security fields, where the development of sensing devices being able to discriminate the enantiomers of potentially harmful substances represents an urgent task. In this context, our focus is to develop chiral chemical sensors based on rationally designed sensing materials, intending to fill the existing gap between the production of enantioselective receptors and the realization of macroscopic devices being able to work in real scenarios. As an example of such sensors, we have recently reported that sensing layers consisting of metalloporphyrins combined with chiral cyclohexanohemicucurbit[8]urils deposited on quartz microbalances efficiently recognize vapor samples of limonene and 1-phenylethylamine enantiomers by application of a novel normalization procedure and multivariate analysis techniques to improve the classification performances.[8] In this paper, we report new chiral nanosystems by integrating porphyrin-based receptors into silica nanohelices. Indeed, nanoscale siliceous materials offer a number of potential advantages for sensing applications, thanks to their stable structural and functional properties,[9−11] also in combination with organic dyes like porphyrins.[12−17] The selectivity toward a target analyte can be tuned by adequately decorating the pore walls and/or channels with porphyrin receptors, giving an easily readable analytical signal thanks to the extraordinary photochemical properties of these macrocycles.

Received: October 28, 2023
Revised: January 4, 2024
Accepted: January 5, 2024
Published: January 31, 2024

Downloaded via UNIVERSITA DI ROMA LA SAPIENZA on June 20, 2024 at 08:39:21 (UTC).
See https://pubs.acs.org/sharingguidelines for options on how to legitimately share published articles.

© 2024 American Chemical Society

https://doi.org/10.1021/acs.jpcb.3c07153
J. Phys. Chem. B 2024, 128, 1550−1556

We have previously reported how achiral gemini-type dialkyl diammonium amphiphilic molecules complexed with chiral tartrate counterions self-assemble to helical nanoribbons. The coverage of these structures with silica gives rise to organic−inorganic chiral nanostructures called hybrid nanohelices (HH, Figure 1a).[18−21] When tartrate anions as an origin of chirality are replaced with other anions, the confinement in the nanometric chiral space given by the solid silica walls may induce a chiroptical activity in the new guest molecules. Thus, hybrid nanohelices provide a versatile chiral nanospace where achiral molecules can enter and organize in a chiral way (see the CD signal of hybrid nanohelices, HH, in Figure 1b).[20,21] In the present work, we extend this approach to study chiral porphyrin derivatives. The environment of these organic macrocycles can be analyzed, thanks to their rich spectroscopic features, which are markedly sensitive to self-aggregation and local microenvironment,[22] such as supramolecular chirogenesis.[23] In addition, having an excellent host−guest complexing ability, it can be used for a variety of selective separations.[24] We selected a set of water-insoluble porphyrins composed of two achiral (H_2P and ZnP) and six chiral [(L)H_2P, (D)H_2P, (L)ZnP, (D)ZnP, HB6U, and ZnB6U] porphyrin derivatives (Figure 1c).

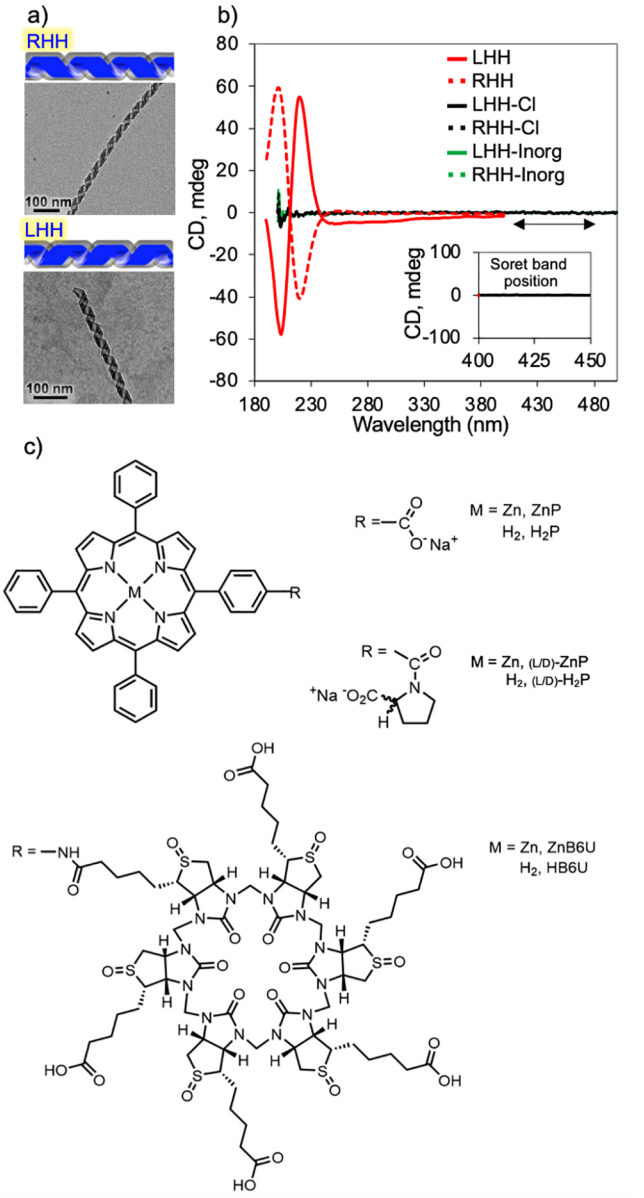

Figure 1. (a) TEM images of right-handed hybrid nanohelices (RHH) and left-handed hybrid nanohelices (LHH), (b) CD signals of different prepared nanostructures based on hybrid silica nanohelices, and (c) structures of achiral ZnP and H_2P and chiral (L or D)-ZnP, (L or D)-H_2P, ZnB6U, and HB6U and guest molecules used in this work, where letters L and D express handedness of chiral porphyrins, Zn stands for zinc metal in metalloporphyrins, and all others are free-base porphyrin derivatives. LHH and RHH represent left-handed helices and right-handed helices, respectively. −Cl and -inorg represent right- or left-handed nanohelices modification.

Since most applications require recognizing chiral target analytes in water or aqueous solutions, such as pollutants or contaminants, the lack of or no solubility in water of most of the porphyrin-based receptors may hinder their practical applications. The incorporation of porphyrin derivatives into water-dispersible silica nanohelices (Figure S1a) allows to overcome this problem, hence enabling their use as chemical probes to detect various analytes in water.

EXPERIMENTAL SECTION

All solvents and chemicals are of the highest purity grade available from Sigma-Aldrich and used without further purification. We previously reported the preparation and self-assembly behavior in solution for porphyrin derivatives ZnP, H_2P, (D/L)ZnP, and (D/L)H_2P.[25] Synthetic procedures for HB6U and ZnB6U are presented in Supporting Information. Transmission electron microscopy (TEM) was performed with a CM 120 (Philips) at 120 kV. For TEM experiments, samples were applied to carbon-coated copper 300 mesh grids. Circular dichroism (CD) and absorption spectra were measured with a J-815 (JASCO) CD spectrometer. FTIR spectra were recorded with a Thermo-Nicolet Nexus 670 FTIR spectrometer, at a resolution of 4 cm^{-1}, by recording 50 scans.

Porphyrin Aggregation Procedure. 1 mM stock solutions (1 mM) were prepared for each porphyrin derivative in the proper organic solvents (DMSO for ZnB6U, THF for HB6U, and DMF for the two enantiomeric pairs of ZnP and H_2P). An aliquot of 200 μL of porphyrins in the respective organic solvent was added to 2.8 mL of water to reproduce the ion exchange protocol. Finally, CD and UV−vis spectra were acquired after 8 h. Due to the intense absorbance of samples, a 1 mm cuvette optical path length was utilized for these experiments to maintain the corresponding optical density below 1.5.

Synthesis of Hybrid Silica Nanohelices Using Chloride. *N*,*N*′-Dihexadecyl-*N*,*N*,*N*′,*N*′-tetramethylethylene diammonium L- (and D-) tartrate (16−2−16 L- (and D-) tartrate) were synthesized by the previously reported procedure.[26−28] The powder of 16−2−16 gemini tartrate was dissolved into water at 60 °C (1 mM) and then aged for 4 days at 20 °C with the typical quantities used being 20 mg of powder for 28 mL of ultrapure water. Then, the 16−2−16 L- or D-tartrate self-assemblies are used as templates to prepare corresponding silica nanostructures like helices through a sol−gel transcription procedure. In a typical preparation, 0.5 mL of tetraethoxysilane (TEOS) was added to 10 mL of 10^{-4} M aqueous solution of D- or L-tartaric acid and prehydrolyzed at 20 °C by stirring on a roller mixer for 7 h. Then, 5 mL of prehydrolyzed TEOS was mixed with 5 mL of organic gel, and the mixture was stirred at 20 °C in a roller mixer overnight.

https://doi.org/10.1021/acs.jpcb.3c07153
J. Phys. Chem. B 2024, 128, 1550−1556

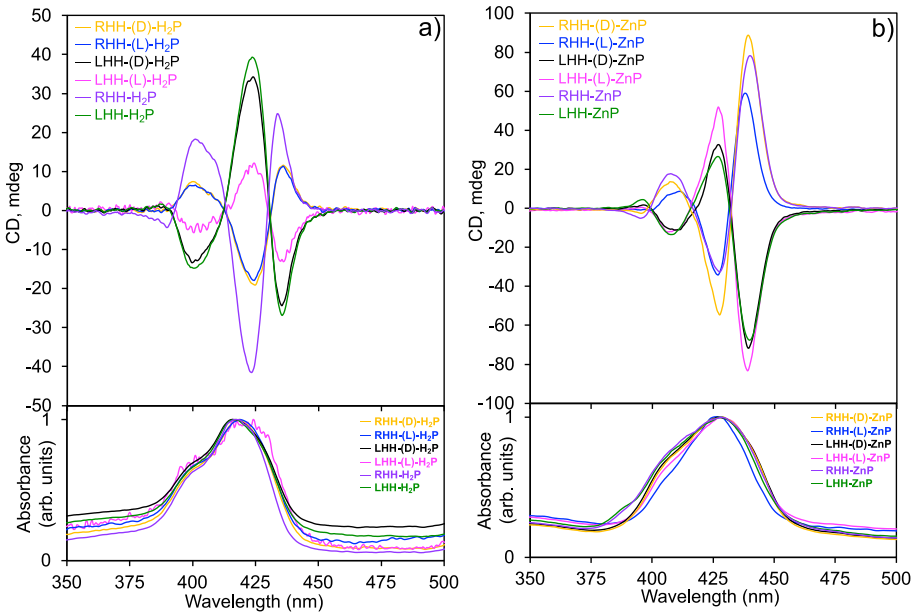

Figure 2. CD and UV−vis spectra obtained from nanostructured porphyrin derivatives (chiral and achiral) with and without different combinations of LHH and RHH. (a,b) CD and normalized absorbance spectra (at the peak position) for free base and zinc-based porphyrins (respectively).

Once the transcription was completed, the mixture was thoroughly washed five times with centrifugation in ultrapure water (4 °C). In order to insert the porphyrins' molecules in the structure, the counterions of D- or L-16−2−16 hybrid silica were first replaced by chloride ions by washing eight times with KCl (100 mM) at 4 °C until no tartrate was detected using CD and followed by washing five times with ultrapure water (4 °C)[29] (Figure 1b). Then, the concentration of prepared right or left hybrid helix chloride (RHH-Cl or LHH-Cl) was adjusted to the desired value (0.5 mg/mL) using ultrapure water and kept at 4 °C.

Porphyrin Molecule Insertion Procedure. To insert porphyrin molecules by ion exchange, we made it interact with hybrid silica helices chloride (RHH-Cl or LHH-Cl) dispersed in water at 20 °C with a molar ratio of 1:1 in THF/H_2O (1:14, v/v) (for HB6U), DMSO/H_2O (1:14, v/v) (for ZnB6U), and DMF/H_2O (1:14, v/v) (for other molecules). Each initial solution contains a 1 mM concentration of a desired molecule in the corresponding solvent. Then, 200 μL of each solution was poured in 2.8 mL of hybrid helices chloride dispersion in water (RHH-Cl or LHH-Cl), and then the mixture was aged for 1 h on a roller mixer at 20 °C, followed by four washings using centrifugation (12 min at 4500 rpm) at 4 °C. The insertion of porphyrin molecules was confirmed using FTIR analysis as presented in Supporting Information (see Figure S2 with discussion).

■ RESULTS AND DISCUSSION

Porphyrins in Solutions. While solubilized in the respective organic solvents as described in the Experimental Section, porphyrins are not aggregated, as evidenced by their spectral invariability. Additionally, even with the presence of chiral appended groups, (L or D)-H_2P and (L or D)-ZnP do not show detectable CD signals in the visible region of the spectra. The addition of an antisolvent, such as water, induces aggregation of the porphyrins, which can lead to the formation of stereospecific supramolecular structures that often display very intense CD signals in the visible region. The aggregation mechanisms and protocols to stereospecifically organized chiral and achiral porphyrins by supramolecular interactions have extensively been investigated.[25,30] The efficiency in chiral induction of these systems depends on many different parameters, such as solvent, concentration, pH, temperature, and even preparation protocol of samples.[31,32] In the present case, as expected, water-induced aggregation of pristine achiral H_2P and ZnP does not show CD signals proving the absence of unwanted potential chiral effectors during the procedure (Table S1). On the other hand, the aggregates of all the chiral porphyrin derivatives herein studied at the same condition show supramolecular CD signals with dissymmetric g-factors (normalized optical activity, which is defined as $\Delta\varepsilon/\varepsilon$) in the range of 10^{-5} (see Table S1 and Figures S3 and S4).

Hybrid Silica Nanohelices with Achiral Porphyrins. In agreement with our previous report, right- (RHH) and left-handed hybrid helices (LHH) (before ion exchange) show mirror-image CD signals at 200−250 nm, which correspond to the tartrate's carboxylic groups (Figure 1b).

When porphyrins are incorporated into the hybrid silica nanohelices via the ion exchange procedure described above, the UV−vis spectra of the hybrid systems display the typical visible features imputable to porphyrins. Additionally, the change in contrast on TEM images with FTIR analysis (Figures S1b and S2) confirms the insertion of porphyrin molecules into the chiral nanospace of hybrid silica nanohelices without modification of the helical morphology of the latter (similar observation was reported in our previous work[20,21]). In the cases for which two achiral porphyrins (namely, H_2P and ZnP) are introduced into the chiral nanospaces of RHH or LHH, the Soret band region shows the CD spectra features with oppositely signed Cotton effects, depending on the handedness of the helices (Figure 2). Thus, RHH-induced exciton-coupled CD shows a +//+ pattern, while in the presence of LHH, the corresponding mirror image CD spectrum was observed (Figure 2). The effect of the presence of a coordination metal ion, Zn^{2+}, was investigated. ZnP in hybrid silica nanohelices shows a slightly lower g-factor

https://doi.org/10.1021/acs.jpcb.3c07153
J. Phys. Chem. B 2024, 128, 1550−1556

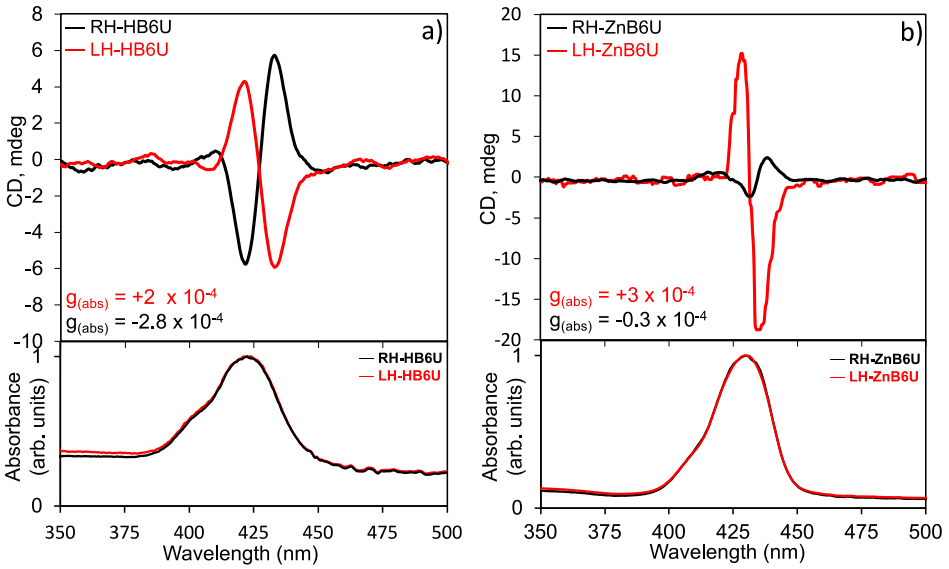

Figure 3. CD and UV−vis spectra obtained from HB6U and ZnB6U molecules with and without different combinations of LHH and RHH. (a,b) CD and normalized absorbance spectra (at the peak position) for free base and zinc-based B6U, respectively.

compared to H_2P in hybrid silica nanohelices (~2.0×10^{-3} for H_2P at 424 nm and ~0.6×10^{-3} for ZnP at 427 nm). Unlike the free base macrocycles, Zn-porphyrins have a possibility to coordinate a ligand axially, and, and the zinc ion has good oxophilicity that may confer an additional interaction mechanism with silica and gemini moieties. This coordination could result in an increased distance between electronic transitions and less favorable dihedral angles for exciton coupling. Hence, these additional interactions may account for the lower *g*-factor.

Hybrid Silica Nanohelices with Chiral Porphyrins. Subsequently, we investigated whether the presence of the chiral proline group covalently attached to the porphyrins [(L)-H_2P, (D)-H_2P, (L)-ZnP, and (D)-ZnP] may influence the overall CD features once inserted into the helices. In this case, it is interesting to note that the chiroptical features of these chiral porphyrins confined into RH- or LHH are determined by the handedness of nanohelices, disregarding the appended proline configuration (Figure 2). This indicates that the effect of the mesoscopic handedness of hybrid silica nanohelices is a determining factor of the CD signals, which predominates over the molecular chirality of porphyrin. Table S1 shows that CD spectra of hybrid porphyrin-silica nanostructures-based chiral/achiral free bases H_2P and ZnP generally have one or 2 orders of magnitude higher *g*-factors of the corresponding supramolecular assembly (from ~5×10^{-4} up to ~2×10^{-3}). In these systems, the crystalline packing of gemini surfactants and the resulting chiral environment inside HH are responsible for the chiral organization of anionic molecules trapped inside, which leads to the appearance or amplification of chirality of the anions, which is in good agreement with our previous reports in which hybrid silica nanohelices were used to induce chirality to various anionic dyes and monoanions.[21,29,33,34] The amplitude of the CD spectra of chiral porphyrins@hybrid silica nanohelices decreases slightly in the case of porphyrin free bases ((L)- or (D)-H_2P), whereas for chiral ZnPs, they are similar to achiral ZnP (*g*-factors ~0.6×10^{-3} for both chiral and achiral ZnP) (see Table S1). Remarkably, the amplification of CD signals by the porphyrins' incorporation into silica nanohelices is much more effective than the aggregation-induced amplification, probably due to the presence of water antisolvent. Apparently, it is due to the chiral arrangement of porphyrins induced by an electrostatic interaction with chiral and crystalline gemini surfactants confined in the chiral nanospace of silica helices as compared to randomly aggregated porphyrins (Table S1).

Hemicucurbituril-Appended Porphyrins. We then studied the system for which the porphyrins (free base and zinc complex) are covalently linked to D-biotin-L-sulfoxide[6]-uril,[35] (B6U) macrocycle,[36] giving mono porphyrin-substituted D-biotin-L-sulfoxide[6]urils (HB6U and ZnB6U, respectively). These systems allow us to investigate the effect of much larger chiral moieties capable of molecular recognition.[37] In addition, porphyrin and B6U have similar dimensions close to a nanometer, making this combination very appealing at the supramolecular level. Both HB6U in THF and ZnB6U in DMSO solutions gave bathochromic shifts of the porphyrin Soret band. These spectral features are similar to the UV−vis absorption reported for zinc porphyrin complexes with enantiopure cyclohexanohemicucurbit[*n*]urils (*n* = 6 and 8).[38] When HB6Us are incorporated inside the chiral nanospace of hybrid silica nanohelices, a noticeable increase of the corresponding *g*-factors (|2−3 × 10^{-4}| (Figure 3) for both RHH and LHH compared to 5 × 10^{-5} for the molecular solution of HB6U, Figures S3 and S4) was observed. The signs of these CD signals adhere to the handedness of the hybrid silica nanohelices, which agrees with what was observed in the case of H_2P (L and D) molecules, again showing that the helical chirality of hybrid silica nanohelices dominates over molecular chirality. For the biotinuril-zincporphyrin macrocycle, ZnB6U, on the other hand, while a similar chirality amplification was observed with LHH, i.e., *g*-factors |3.0 × 10^{-4}|, the observed CD signal shows very little amplification with RHH, |3 × 10^{-5}| (Figures 3 and S4). The number of HB6U and ZnB6U molecules interacting with the RHH and LHH chiral templates was quantified by recording the UV−vis absorbance of supernatant solutions after the functionalization process (Figure S5). About 3.2 × 10^{-7} moles of HB6U is incorporated in 1 mg of hybrid silica nanohelices (corresponding to 1.6 × 10^{-6} moles of gemini surfactants) both for RHH and LHH. A

https://doi.org/10.1021/acs.jpcb.3c07153
J. Phys. Chem. B 2024, 128, 1550−1556

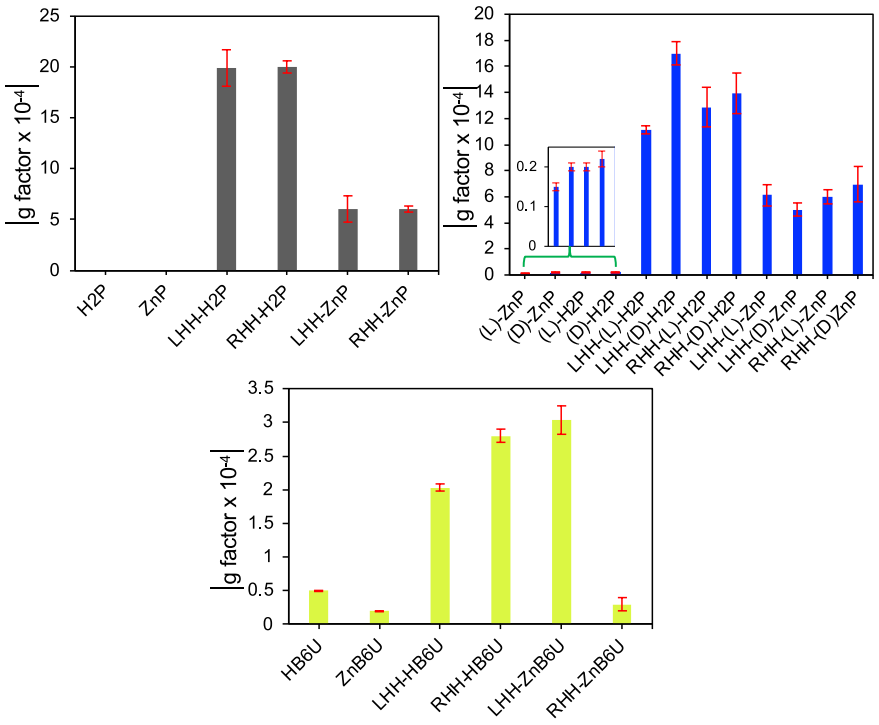

Figure 4. Comparison of *g*-factors (at 420−425 nm) of studied systems with (a) achiral porphyrin (H_2P and ZnP), (b) chiral porphyrin ((D or L)-H_2P and (D or L)-ZnP), and (c) hemicucurbituril appended porphyrin (HB6U and ZnB6U).

similar value of the occupancy was observed for ZnB6U bound to LHH. On the other hand, in the case of the ZnB6U-RHH system, only 1.0×10^{-7} moles of ZnB6U was incorporated, suggesting that ZnB6U molecule has much weaker interaction with RHH. Such results suggest that while the chiral moieties of HB6U have little effect on the organization of the porphyrins in the chiral nanospace of the helices, ZnB6U has a different organization in LHH or in RHH. This is again probably due to the lower in-plane flexibility of Zn porphyrin, which results in the B6U moieties being more intimately linked with the Zn porphyrin, and having an additional interaction with the silica and gemini moieties.[39,40] Nevertheless, the *g*-factor amplification is rather modest for the B6U complex with a helix, compared to smaller porphyrins, as shown in Figure 4a,b. We suggest that the relatively large biotinuril macrocycle suppresses the ability of porphyrins to penetrate hybrid silica nanohelices. Clearly, in the case of ZnB6U, additional interactions by zinc cation have an effect on diastereoselective binding to the inorganic helix. This highlights the generation of the matching effect between ZnB6U and the LH helix (larger *g*-factor), whereas the mismatching impact can be seen with RHH (lower *g*-factor) (Figure 4c).

The ensemble of the *g*-factors (measured at 420−425 nm) observed from the Soret bands of porphyrins as described above is summarized in Figure 4.

CONCLUSIONS

In this work, we demonstrated that the chiral nanoenvironment, the absolute configuration, and the nature of porphyrin molecules cooperatively affect the chirality amplification process upon confinement in the chiral nanospace of hybrid silica nanohelices.

Both chiral and achiral porphyrins [(L or D)-H_2P, (L or D)-ZnP, H_2P, and ZnP] confined in hybrid silica nanohelices show opposite Cotton effects at the corresponding Soret band, the sign of which is determined solely by the handedness of hybrid silica nanohelices. The amplification of the *g*-factors due to the aggregation of porphyrin derivatives in the nanohelical environment was largely dominant with respect to the molecular chirality being negligible. Indeed, the *g*-factors of (L or D)-H_2P, (L or D)-ZnP increased by 25−80 times when they are incorporated in the nanohelices compared to when they are free in solution.

The chirality amplification was more efficient for achiral and free base porphyrins compared to chiral and Zn complex counterparts. Zn ions may coordinate some external (achiral) ligands that can enlarge the distance between the electronic transitions and/or make the dihedral angles less favorable for exciton coupling. For the covalently linked biotinuril-porphyrins, the chirality amplification was again more efficient for the free-base porphyrins HB6U and the induced CD signals were dependent only on the handedness of the hybrid silica nanohelices. Interestingly, for ZnB6U, the chirality amplification was observable only for LHH, while no chirality amplification was found in the case of RHH with much less incorporated amount of ZnB6U (<25%).

The smaller the anionic moieties, the higher the chirality amplification, with free base porphyrins showing stronger amplification. As a consequence, the order of chiral amplification is follows: H_2P@HH > (L)-H_2P@HH or (D)-H_2P@HH > ZnP@HH > (L)-ZnP@HH or (D)-ZnP@HH > HB6U@HH ≈ matched ZnB6U@HH ≫ mismatched ZnB6U@HH ≈ chiral H_2P in solution ≈ chiral ZnP in solution; HH represents "hybrid silica nanohelices".

The ensemble of the data indicates that two factors may be the dominant origin of chirality induction to porphyrins. The first is the flexibility of the confined porphyrin ring, which influences the ability of the ring to accommodate the chiral induction enforced by the chiral environment. The second is an exciton coupling of the corresponding electronic transitions.

https://doi.org/10.1021/acs.jpcb.3c07153
J. Phys. Chem. B 2024, 128, 1550−1556

In the case of the second effect, the distance and dihedral angle between the coupling electronic transitions are the main controlling factors.

The structural deviation of porphyrin can induce changes in the spatial, physical, and electronic structure, which in turn can change its electronic transitions and properties, thus leading to differences in interaction with hybrid silica nanohelices. Such an observation can shed light on how chiral molecules organize and assemble into chiral nanospace, resulting in induction and amplification of their chiroptical behaviors, and can help the design of new chiral hybrid systems based on porphyrin and robust inorganic nanostructures for specific chiral applications.

■ ASSOCIATED CONTENT

Supporting Information

The Supporting Information is available free of charge at https://pubs.acs.org/doi/10.1021/acs.jpcb.3c07153.

Schematic presentation of porphyrins in chiral nanospaces, UV−vis, CD signals and *g*-factors, and TEM characterization of nanostructures with porphyrins (PDF)

■ AUTHOR INFORMATION

Corresponding Author

Reiko Oda − *University of Bordeaux, CNRS, Bordeaux INP, CBMN, Pessac 33600, France; WPI-Advanced Institute for Materials Research, Tohoku University, Aoba-Ku, Sendai 980-8577, Japan;* orcid.org/0000-0003-3273-8635; Email: reiko.oda@u-bordeaux.fr

Authors

Zakaria Anfar − *University of Bordeaux, CNRS, Bordeaux INP, CBMN, Pessac 33600, France;* orcid.org/0000-0001-8840-7160

Balamurugan Kuppan − *University of Bordeaux, CNRS, Bordeaux INP, CBMN, Pessac 33600, France*

Antoine Scalabre − *University of Bordeaux, CNRS, Bordeaux INP, CBMN, Pessac 33600, France*

Rahul Nag − *University of Bordeaux, CNRS, Bordeaux INP, CBMN, Pessac 33600, France*

Emilie Pouget − *University of Bordeaux, CNRS, Bordeaux INP, CBMN, Pessac 33600, France;* orcid.org/0000-0002-3175-6201

Sylvain Nlate − *University of Bordeaux, CNRS, Bordeaux INP, CBMN, Pessac 33600, France*

Gabriele Magna − *Department of Chemical Science and Technologies, University of Rome Tor Vergata, Rome 00133, Italy;* orcid.org/0000-0003-2140-0110

Ilaria Di Filippo − *Department of Chemical Science and Technologies, University of Rome Tor Vergata, Rome 00133, Italy*

Donato Monti − *Department of Chemistry, Sapienza, University of Rome, Rome 00185, Italy*

Mario L. Naitana − *Department of Chemical Science and Technologies, University of Rome Tor Vergata, Rome 00133, Italy*

Manuela Stefanelli − *Department of Chemical Science and Technologies, University of Rome Tor Vergata, Rome 00133, Italy;* orcid.org/0000-0001-8563-8043

Tatsiana Nikonovich − *Department of Chemistry and Biotechnology, School of Science, Tallinn University of Technology, Tallinn 12618, Estonia*

Victor Borovkov − *Department of Chemistry and Biotechnology, School of Science, Tallinn University of Technology, Tallinn 12618, Estonia;* orcid.org/0000-0001-7898-0457

Riina Aav − *Department of Chemistry and Biotechnology, School of Science, Tallinn University of Technology, Tallinn 12618, Estonia;* orcid.org/0000-0001-6571-7596

Roberto Paolesse − *Department of Chemical Science and Technologies, University of Rome Tor Vergata, Rome 00133, Italy;* orcid.org/0000-0002-2380-1404

Complete contact information is available at: https://pubs.acs.org/10.1021/acs.jpcb.3c07153

Author Contributions

The manuscript was written through contributions of all authors. All authors have given approval to the final version of the manuscript.

Notes

The authors declare no competing financial interest.

■ ACKNOWLEDGMENTS

Funding: Estonian Research Council grant PRG399 and European Union's H2020- FET-OPEN grant 828779 (INITIO).

■ REFERENCES

(1) Niu, X.; Zhao, R.; Yan, S.; Pang, Z.; Li, H.; Yang, X.; Wang, K. Chiral Materials: Progress, Applications, and Prospects. *Small* **2023**, *19*, 2303059.

(2) Xia, Y.; Zhou, Y.; Tang, Z. Chiral Inorganic Nanoparticles: Origin, Optical Properties and Bioapplications. *Nanoscale* **2011**, *3* (4), 1374.

(3) Lv, J.; Gao, X.; Han, B.; Zhu, Y.; Hou, K.; Tang, Z. Self-Assembled Inorganic Chiral Superstructures. *Nat. Rev. Chem* **2022**, *6* (2), 125−145.

(4) Duan, Y.; Che, S. Chiral Mesostructured Inorganic Materials with Optical Chiral Response. *Adv. Mater.* **2023**, *35*, 2205088.

(5) Dong, Y.; Zhang, Y.; Li, X.; Feng, Y.; Zhang, H.; Xu, J. Chiral Perovskites: Promising Materials toward Next-Generation Optoelectronics. *Small* **2019**, *15* (39), 1902237.

(6) Wang, F.; Yue, X.; Ding, Q.; Lin, H.; Xu, C.; Li, S. Chiral Inorganic Nanomaterials for Biological Applications. *Nanoscale* **2023**, *15* (6), 2541−2552.

(7) Xiao, X.; Chen, C.; Zhang, Y.; Kong, H.; An, R.; Li, S.; Liu, W.; Ji, Q. Chiral Recognition on Bare Gold Surfaces by Quartz Crystal Microbalance. *Angew. Chem.* **2021**, *133* (47), 25232−25237.

(8) Magna, G.; Šakarašvili, M.; Stefanelli, M.; Giancane, G.; Bettini, S.; Valli, L.; Ustrnul, L.; Borovkov, V.; Aav, R.; Monti, D.; et al. Chiral Recognition by Supramolecular Porphyrin-Hemicucurbit[8]Uril-Functionalized Gravimetric Sensors. *ACS Appl. Mater. Interfaces* **2023**, *15* (25), 30674−30683.

(9) Walcarius, A.; Mercier, L. Mesoporous Organosilica Adsorbents: Nanoengineered Materials for Removal of Organic and Inorganic Pollutants. *J. Mater. Chem.* **2010**, *20* (22), 4478.

(10) Flores, D.; Almeida, C. M. R.; Gomes, C. R.; Balula, S. S.; Granadeiro, C. M. Tailoring of Mesoporous Silica-Based Materials for Enhanced Water Pollutants Removal. *Molecules* **2023**, *28* (10), 4038.

(11) Parra, M.; Gil, S.; Gaviña, P.; Costero, A. M. Mesoporous Silica Nanoparticles in Chemical Detection: From Small Species to Large Bio-Molecules. *Sensors* **2021**, *22* (1), 261.

(12) Radi, S.; Abiad, C. E.; Moura, N. M. M.; Faustino, M. A. F.; Neves, M. G. P. M. S. New Hybrid Adsorbent Based on Porphyrin Functionalized Silica for Heavy Metals Removal: Synthesis, Characterization, Isotherms, Kinetics and Thermodynamics Studies. *J. Hazard. Mater.* **2019**, *370*, 80−90.

(13) Hu, M.; Kang, W.; Zhong, Z.; Cheng, B.; Xing, W. Porphyrin-Functionalized Hierarchical Porous Silica Nanofiber Membrane for Rapid HCl Gas Detection. *Ind. Eng. Chem. Res.* **2018**, *57* (34), 11668−11674.
(14) Anghel, D.; Lascu, A.; Epuran, C.; Fratilescu, I.; Ianasi, C.; Birdeanu, M.; Fagadar-Cosma, E. Hybrid Materials Based on Silica Matrices Impregnated with Pt-Porphyrin or PtNPs Destined for CO2 Gas Detection or for Wastewaters Color Removal. *Int. J. Mol. Sci.* **2020**, *21* (12), 4262.
(15) Osica, I.; Imamura, G.; Shiba, K.; Ji, Q.; Shrestha, L. K.; Hill, J. P.; Kurzydłowski, K. J.; Yoshikawa, G.; Ariga, K. Highly Networked Capsular Silica-Porphyrin Hybrid Nanostructures as Efficient Materials for Acetone Vapor Sensing. *ACS Appl. Mater. Interfaces* **2017**, *9* (11), 9945−9954.
(16) Muduganti, M.; Magna, G.; di Zazzo, L.; Stefanelli, M.; Capuano, R.; Catini, A.; Duranti, L.; Di Bartolomeo, E.; Sivalingam, Y.; Bernardini, S.; et al. Porphyrinoids Coated Silica Nanoparticles Capacitive Sensors for COVID-19 Detection from the Analysis of Blood Serum Volatolome. *Sensors Actuators B Chem.* **2022**, *369*, 132329.
(17) Marcelo, G. A.; Pires, S. M. G.; Faustino, M. A. F.; Simões, M. M.; Neves, M. P.; Santos, H. M.; Capelo, J. L.; Mota, J. P.; Lodeiro, C.; Oliveira, E. New Dual Colorimetric/Fluorimetric Probes for Hg2+ Detection & Extraction Based on Mesoporous SBA-16 Nanoparticles Containing Porphyrin or Rhodamine Chromophores. *Dyes Pigm.* **2019**, *161*, 427−437.
(18) Okazaki, Y.; Buffeteau, T.; Siurdyban, E.; Talaga, D.; Ryu, N.; Yagi, R.; Pouget, E.; Takafuji, M.; Ihara, H.; Oda, R. Direct Observation of Siloxane Chirality on Twisted and Helical Nanometric Amorphous Silica. *Nano Lett.* **2016**, *16* (10), 6411−6415.
(19) Pranee, P.; Scalabre, A.; Labrugere, C.; Ryu, N.; Yano, A.; Hano, N.; Talaga, D.; Okazaki, Y.; Pouget, E.; Nlate, S.; et al. Sequential Chiral Induction between Organic and Inorganic Supramolecular Helical Assemblies for the in Situ Formation of Chiral Carbon Dots. *Chem. Commun.* **2023**, *59* (64), 9762−9765.
(20) Duroux, G.; Robin, L.; Liu, P.; Dols, E.; Mendes, M. D. S. L.; Buffière, S.; Pardieu, E.; Scalabre, A.; Buffeteau, T.; Nlate, S.; et al. Induced Circular Dichroism from Helicoidal Nano Substrates to Porphyrins: The Role of Chiral Self-Assembly. *Nanoscale* **2023**, *15* (28), 12095−12104.
(21) Scalabre, A.; Okazaki, Y.; Kuppan, B.; Buffeteau, T.; Caroleo, F.; Magna, G.; Monti, D.; Paolesse, R.; Stefanelli, M.; Nlate, S.; et al. Chirality Induction to Achiral Molecules by Silica-coated Chiral Molecular Assemblies. *Chirality* **2021**, *33* (9), 494−505.
(22) Occhiuto, I.; De Luca, G.; Villari, V.; Romeo, A.; Micali, N.; Pasternack, R. F.; Scolaro, L. M. Supramolecular Chirality Transfer to Large Random Aggregates of Porphyrins. *Chem. Commun.* **2011**, *47* (21), 6045.
(23) Borovkov, V. V.; Hembury, G. A.; Inoue, Y. Origin, Control, and Application of Supramolecular Chirogenesis in Bisporphyrin-Based Systems. *Acc. Chem. Res.* **2004**, *37* (7), 449−459.
(24) Ogoshi, T.; Yamagishi, T.; Nakamoto, Y. Pillar-Shaped Macrocyclic Hosts Pillar[n]Arenes: New Key Players for Supramolecular Chemistry. *Chem. Rev.* **2016**, *116* (14), 7937−8002.
(25) Stefanelli, M.; Savioli, M.; Zurlo, F.; Magna, G.; Belviso, S.; Marsico, G.; Superchi, S.; Venanzi, M.; Di Natale, C.; Paolesse, R.; et al. Porphyrins Through the Looking Glass: Spectroscopic and Mechanistic Insights in Supramolecular Chirogenesis of New Self-Assembled Porphyrin Derivatives. *Front. Chem.* **2020**, *8*, 587842.
(26) Oda, R.; Huc, I.; Candau, S. J. Gemini Surfactants as New, Low Molecular Weight Gelators of Organic Solvents and Water. *Angew. Chem., Int. Ed.* **1998**, *37* (19), 2689−2691.
(27) Okazaki, Y.; Cheng, J.; Dedovets, D.; Kemper, G.; Delville, M.-H.; Durrieu, M.-C.; Ihara, H.; Takafuji, M.; Pouget, E.; Oda, R. Chiral Colloids: Homogeneous Suspension of Individualized SiO 2 Helical and Twisted Nanoribbons. *ACS Nano* **2014**, *8* (7), 6863−6872.
(28) Brizard, A.; Aimé, C.; Labrot, T.; Huc, I.; Berthier, D.; Artzner, F.; Desbat, B.; Oda, R. Counterion, Temperature, and Time Modulation of Nanometric Chiral Ribbons from Gemini-Tartrate Amphiphiles. *J. Am. Chem. Soc.* **2007**, *129* (12), 3754−3762.
(29) Okazaki, Y.; Ryu, N.; Buffeteau, T.; Pathan, S.; Nagaoka, S.; Pouget, E.; Nlate, S.; Ihara, H.; Oda, R. Induced Circular Dichroism of Monoatomic Anions: Silica-Assisted the Transfer of Chiral Environment from Molecular Assembled Nanohelices to Halide Ions. *Chem. Commun.* **2018**, *54* (73), 10244−10247.
(30) Stefanelli, M.; Magna, G.; Di Natale, C.; Paolesse, R.; Monti, D. Stereospecific Self-Assembly Processes of Porphyrin-Proline Conjugates: From the Effect of Structural Features and Bulk Solvent Properties to the Application in Stereoselective Sensor Systems. *Int. J. Mol. Sci.* **2022**, *23* (24), 15587.
(31) Magna, G.; Monti, D.; Di Natale, C.; Paolesse, R.; Stefanelli, M. The Assembly of Porphyrin Systems in Well-Defined Nanostructures: An Update. *Molecules* **2019**, *24* (23), 4307.
(32) Zhang, L.; Wang, T.; Jiang, J.; Liu, M. Chiral Porphyrin Assemblies. *Aggregates* **2023**, *4* (1), 198.
(33) Ryu, N.; Okazaki, Y.; Hirai, K.; Takafuji, M.; Nagaoka, S.; Pouget, E.; Ihara, H.; Oda, R. Memorized Chiral Arrangement of Gemini Surfactant Assemblies in Nanometric Hybrid Organic-Silica Helices. *Chem. Commun.* **2016**, *52* (34), 5800−5803.
(34) Álvaro-Martins, M. J.; Garcés-Garcés, J.; Scalabre, A.; Liu, P.; Fernández-Lázaro, F.; Sastre Santos, C.; Bassani, D. M.; Oda, R. Disentangling Excimer Emission from Chiral Induction in Nanoscale Helical Silica Scaffolds Bearing Achiral Chromophores. *ChemPhysChem* **2023**, *24* (90), No. e202200573.
(35) Andersen, N. N.; Eriksen, K.; Lisbjerg, M.; Ottesen, M. E.; Milhøj, B. O.; Sauer, S. P. A.; Pittelkow, M. Entropy/Enthalpy Compensation in Anion Binding: Biotin[6]uril and Biotin-l-sulfoxide[6]uril Reveal Strong Solvent Dependency. *J. Org. Chem.* **2019**, *84* (5), 2577−2584.
(36) Lisbjerg, M.; Jessen, B. M.; Rasmussen, B.; Nielsen, B. E.; Madsen, A. Ø.; Pittelkow, M. Discovery of a cyclic 6 + 6 hexamer of d-biotin and formaldehyde. *Chem. Sci.* **2014**, *5* (7), 2647−2650.
(37) Aav, R.; Mishra, K. The Breaking of Symmetry Leads to Chirality in Cucurbituril-Type Hosts. *Symmetry* **2018**, *10* (4), 98.
(38) Ustrnul, L.; Kaabel, S.; Burankova, T.; Martõnova, J.; Adamson, J.; Konrad, N.; Burk, P.; Borovkov, V.; Aav, R. Supramolecular Chirogenesis in Zinc Porphyrins by Enantiopure Hemicucurbit[n]-Urils (n = 6, 8). *Chem. Commun.* **2019**, *55* (96), 14434−14437.
(39) Cheng, B.; Munro, O. Q.; Marques, H. M.; Scheidt, W. R. An Analysis of Porphyrin Molecular FlexibilityUse of Porphyrin Diacids. *J. Am. Chem. Soc.* **1997**, *119* (44), 10732−10742.
(40) Winters, M. U.; Kärnbratt, J.; Eng, M.; Wilson, C. J.; Anderson, H. L.; Albinsson, B. Photophysics of a Butadiyne-Linked Porphyrin Dimer: Influence of Conformational Flexibility in the Ground and First Singlet Excited State. *J. Phys. Chem. C* **2007**, *111* (19), 7192−7199.

https://doi.org/10.1021/acs.jpcb.3c07153
J. Phys. Chem. B 2024, 128, 1550−1556